Articles

Design and Synthesis of Bipyridyl-Containing Conjugated Polymers: Effects of Polymer Rigidity on Metal Ion Sensing

Bin Liu,[†] Wang-Lin Yu,[†] Jian Pei,[†] Shao-Yong Liu,[†] Yee-Hing Lai,*[,‡] and Wei Huang*[,†,§]

Institute of Materials Research and Engineering (IMRE), National University of Singapore, 3 Research Link, Singapore 117602, Republic of Singapore; and Department of Chemistry, National University of Singapore, 10 Kent Ridge Crescent, Singapore 117543, Republic of Singapore

Received April 16, 2001; Revised Manuscript Received July 31, 2001

ABSTRACT: Three conjugated polymers comprised of 9,9-dioctylfluorene and 2,2′-bipyridine, which are alternatively linked by the C−C single bond (**P1**), vinylene bond (**P2**), or ethynylene bond (**P3**), have been synthesized via the Suzuki reaction, the Wittig−Horner reaction, and the Heck reaction, respectively. The optical, electrochemical, and other physical properties of the polymers are dependent on the linkers. The polymer linked by the C−C single bond exhibits a much larger Stokes shift compared with the other two polymers, indicative of higher extended and rigid backbone conformations in the polymers linked by the vinylene and ethynylene bonds. All the three polymers are sensitive to the existence of a variety of transition metal ions due to the chelation between the 2,2′-bipyridyl moieties and the metal ions. For the metal ions which have moderate and weak coordination ability with the 2,2′-bipyridyl moieties, an obvious difference in response sensitivity is observed among the three polymers: **P1** has the highest sensitivity, which is followed by **P2**, and **P3** always exhibits the lowest sensitivity. The different sensing sensitivity is attributed to the different backbone rigidity of the three polymers, which is caused by the three different linkers. The results suggest the use of C−C single bond linker in the molecular design toward the 2,2′-bipyridyl-based conjugated polymer chemosensors for achieving higher sensing sensitivity.

Introduction

A chemosensor is a molecular system for which the physicochemical properties change upon interaction with a chemical species in such a way as to produce a detectable signal.[1] The construction of a useful molecular-based sensory material generally requires a reversible recognition element and a reporter, so that the changes in color, emission, or even the redox potential are reflected to a certain recognition event.[2] In the past few years, a large number of chemosensors have been devised for the detection of alkali and transition metal ions in solution.[3] Among them, the conjugated polymer-based chemosensors have attracted considerable attention because they offer a myriad of opportunities to couple analyte receptor interactions, as well as nonspecific interactions, into an observed response.[4] In comparison with the conventional molecular-based fluorescent chemosensors, conjugated polymer-based chemosensors have shown enhanced sensitivity through the sensory signal amplification.[5] This concept was first established by Swager et al., through a supposed theory that the receptors are interconnecting as a molecular wire, in which the energy migration may occur along the polymer backbone upon the excitations due to the conductivity of the backbone.[5a] Consequently, the polyreceptor system produces a response larger than that afforded by a small interaction in an analogous small monoreceptor system.[5b]

When azacrown or crown ethers have been used as receptors, the underlying principle of ion-induced conductivity fluctuations either by lowering charge carrier mobility (electrostatic effect) or by destroying the conjugation of the polymers (conformational effect) is clearly illustrated.[6] However, they are only limited to the alkali metal ions with the selectivity depending on the size matching between metal ions and the inner diameter of the receptors. Bipyridyl-based ligands, which have coordinative abilities to a large amount of metal ions, are also attractive recognition receptors, especially for transition metal ions.[7] Wasielewski et al. reported two bipyridyl-containing PPV derivatives, in which the bipyridyl unit was incorporated for every one and three phenylene−vinylene units, respectively.[7a] Different transition metal ions were demonstrated to be chelated by the bipyridyl units in the polymer backbones, which resulted in metal ion-dependent ionochromic effects in the absorption and emission spectra. Theoretical calculations suggested a ca. 20° dihedral angle between two adjacent pyridyl rings in their polymers.[7a] Chelating with the metal ions forced the bipyridyl units to become more planar and thus resulted in an increase of conjugation of the entire polymer chain, leading to the absorption red shift. It is now well

* Corresponding author.
[†] Institute of Materials Research and Engineering (IMRE), National University of Singapore.
[‡] Department of Chemistry, National University of Singapore.
[§] Telephone: (65) 874 8592. Fax: (65) 872 0785. E-mail: wei-huang@imre.org.sg.

10.1021/ma0106651 CCC: $20.00
Published on Web 10/09/2001

accepted that, for bipyridyl-containing polymers, the conformational changes in the backbone play the most important role in producing the observed effects, although some other factors, such as the electron density and the electronic structures of metal ions also need to be considered.[7a,8]

To form bipyridyl-based conjugated polymer chemosensors, the bipyridyl units must be linked with other conjugated units through one of the three linkers, the C−C single bond, the vinylene bond, or the ethynylene bond. Different linkers will result in differences in extension and rigidity of backbones of the resulting polymers. The rotation of the C−C bond connecting the two pyridine rings upon chelation with metal ions will be more or less affected by the difference in backbone extension and rigidity caused by the different linkers. It is thus essential to understand the effect of the three possible chemical bonds on the sensory properties of the resultant polymers. On the other hand, the detection signals of the conjugated polymer-based fluorescent chemosensors are reported to have different fluorescent spectral changes upon interaction with specific ions.[6,7] It is expected that the sensitivity and selectivity of the conjugated polymer-based fluorescent chemosensors should be in association with the intrinsic electronic structures of the conjugated polymers, which are dependent on the backbone structure and the attachment of the side chains.

In this paper, we present three conjugated polymers, basically composed of alternating 2,2′-bipyridyl and fluorene moieties, and their application in sensing metal ions. The polymers are specially designed to link the alternating fluorene and bipyridyl moieties with C−C single, vinylene, and ethynylene bonds, respectively. The structure features allow us to realize different electronic properties by using the same sensing site and the comonomer components. In addition, this design provides us an opportunity to study the effect of polymer backbone extension and rigidity of the conjugated polymer-based chemosensors on the sensitivity and selectivity in metal ions sensing.

Materials and Methods

Instruments. All new compounds were characterized by ^{1}H NMR, ^{13}C NMR, and elemental analysis. NMR spectra were collected on a Bruker ACF 300 spectrometer with chloroform-*d* or DMSO-*d* as the solvent and tetramethylsilane as the internal standard. Melting points (mp) were measured in an Electrothermal IA 9300 Digital melting-point apparatus, and were uncorrected. Thermogravimetric analyses (TGA) were conducted on a Du Pont Thermal Analyst 2100 system with a TGA 2950 thermogravimetric analyzer under a heating rate of 20 °C/min and a nitrogen flow rate of 70 mL/min. Differential scanning calorimetry (DSC) was run on a Du Pont DSC 2910 Module in conjunction with the Du Pont Thermal Analyst system at a heating rate of 20 °C/min. Elemental microanalyses were carried out by the Microanalysis Lab of the National University of Singapore. Cyclic voltammetry (CV) was performed on an EG&G Parc model 273A potentiostat/galvanostat system with a three-electrode cell in a solution of Bu_4NClO_4 (0.10 M) in acetonitrile at a scan rate of 50 mV/s. GPC analysis was conducted with a Waters 2696 separation module equipped with a Waters 410 differential refractometer HPLC system and Waters Styragel HR 4E columns using polystyrene as standard and THF as eluant.

Materials. Reagents and chemicals were purchased from Aldrich Chemical Co. unless otherwise stated.

5,5′-Dibromo-2,2′-bipyridine, 1.[9] Hydrogen bromide gas was passed through an anhydrous methanolic solution of bipyridine (5.12 g, 20 mmol) for 1 h. The precipitate formed (6.02 g, 90%) was collected and dried in a vacuum. In a typical bromination procedure, the crude precipitate (3.37 g, 10 mmol) and bromine (3.20 g, 20 mmol) were heated to 180 °C in a sealed tube for 72 h. The mixture was then allowed to cool, and the solid was treated with sodium sulfite to remove the unreacted bromine. The mixture was then basified with sodium hydroxide. The resulting aqueous solution was extracted with methylene chloride. After removal of the solvent, the crude product was obtained which was further purified by twice recrystallization from chloroform to afford 1.10 g (Y: 35%) of compound **1** as white crystals. Mp: 220.1−221.0 °C. ^{1}H NMR ($CDCl_3$, 300 MHz, ppm): δ 8.70−8.69 (d, 2H, J = 2.40 Hz), 8.30−8.27 (d, 2H, J = 8.82 Hz), 7.95−7.91 (dd, 2H, J = 8.64 Hz, J = 2.22 Hz). Anal. Calcd for $C_{10}H_6N_2Br_2$: C, 38.25; H, 1.93; N, 8.92. Found: C, 38.02; H, 1.94; N, 8.29.

5,5′-Dimethyl-2,2′-bipyridine, 2.[10] Compound **2** was synthesized through self-coupling of 3-picolines catalyzed by the Raney nickel. The product was collected by filtration and recrystallized from diethyl ether to give colorless crystals (yield: 24%). Mp: 115−116 °C. MS (EI, *m*/*z*): 184. ^{1}H NMR ($CDCl_3$, 300 MHz, ppm): δ 8.48 (s, 2H,), 8.23 (dd, 2H, J = 8.13 Hz), 7.60 (dd, 2H, J = 8.25 Hz), 2.38 (s, 6H). Anal. Calcd for $C_{12}H_{12}N_2$: C, 78.23; H, 6.57; N, 15.21. Found: C, 78.31; H, 6.28; N, 15.29.

5,5′-Bis(bromomethyl)-2,2′-bipyridine, 3.[11] 5,5′-Dimethyl-2, 2′-bipyridine (11.05 g, 60.0 mmol), NBS (23.50 g, 132.0 mmol), and a catalytic amount of benzoyl peroxide (BPO) were mixed in tetrachloromethane (600 mL). The mixture was refluxed for 5 h. After the reaction mixture cooled to room temperature, it was extracted with chloroform several times. The organic phase was washed with water and brine and then dried over anhydrous magnesium sulfate. After filtration and solvent evaporation, the residual solid was recrystallized from chloroform to give 9.19 g (yield: 45%) of compound **3** as colorless crystals. Mp: 207−208 °C. MS (EI, *m*/*z*): 342. ^{1}H NMR ($CDCl_3$, 300 MHz, ppm): δ 8.72 (s, 2H), 8.44 (d, 2H, J = 8.35 Hz), 7.89 (dd, 2H, J = 8.35 Hz), 4.58 (s, 4H). Anal. Calcd for $C_{12}H_{10}Br_2N_2$: C, 42.14; H, 2.95; Br, 46.72; N, 8.19. Found: C, 42.05; H, 3.03; Br, 47.85; N, 8.24.

5,5′-Bis(diethylphosphinatyl methyl)-2,2′-bipyridine, 4.[12] The mixture of 5,5′-bis(bromomethyl)-2,2′-bipyridine (1.71 g, 5 mmol) and triethyl phosphite (2.50 g, 15 mmol) was stirred at 125 °C for 4 h. Excess triethyl phosphite was distilled, and the residue was recrystallized from chloroform and hexane to give 1.83 g (yield: 80%) of compound **4** as white crystals. Mp: 109.0−109.9 °C. Anal. Calcd for $C_{20}H_{30}N_2O_6P_2$: C, 52.63; H, 6.62; N, 6.14; P, 13.57. Found: C, 52.34; H, 6.06; N, 6.04; P, 12.25.

2,7-Bis(bromomethyl)-9,9-dioctylfluorene, 5.[13] A mixture of 9,9-dioctylfluorene (7.60 g, 20 mmol), paraformaldehyde (6.02 g, 200 mmol), and 30% of hydrogen bromide in acetic acid (35 mL) was stirred at 60 °C for 24 h. After the reaction mixture cooled to room temperature, it was slowly poured into saturated sodium bicarbonate aqueous solution (200 mL). The mixture was extracted three times with dichloromethane (200 mL) and washed sequentially with water and saturated aqueous sodium bicarbonate solution and brine. The combined organic extracts were dried over anhydrous magnesium sulfate and filtered. After removal of the solvent, sticky brown oil was obtained which was used without further purification.

2,7-Bis(methyleneacetate)-9,9-dioctylfluorene, 6.[14] A mixture of the crude compound **5** (8.64 g, 15 mmol), anhydrous potassium acetate (4.40 g, 45 mmol), and acetic acid anhydride (2.5 mL) in acetic acid (85 mL) was refluxed for 24 h. After it cooled to room temperature, most of the acetic acid was removed under reduced pressure. The residue was poured into water (100 mL), and extracted with ethyl acetate three times. The organic phase was sequentially washed with 5% sodium bicarbonate, water, and brine and then dried over anhydrous magnesium sulfate. After removal of the solvent, the residue was purified by column flushing using hexane and ethyl acetate (100:8) to afford 2.52 g (yield: 32%) of compound **6** as a viscous oil. ^{1}H NMR ($CDCl_3$, 300 MHz, ppm): δ 7.68−7.66 (d, 2H, J = 7.65 Hz), 7.34−7.31 (m, 4H), 5.18 (s, 4H), 2.12 (s, 6H), 1.97−1.92 (m, 4H, J = 4.11 Hz), 1.23−1.05 (m, 20 H),

0.84−0.79 (t, 6H, J = 6.84 Hz), 0.65−0.63 (br, 4H). Anal. Calcd for $C_{35}H_{50}O_4$: C, 78.65; H, 9.36. Found: C, 78.55; H, 9.20.

2,7-Bishydroxymethyl-9,9-dioctylfluorene, 7. Compound **6** (3.74 g, 7 mmol) in THF (70 mL) was added dropwise into a mixture of THF (30 mL) containing lithium aluminum hydride (2.66 g, 70 mmol). The mixture was kept gently refluxing for 8 h with stirring. After the mixture was cooled to room temperature, saturated sodium sulfate solution was added dropwise until the excess lithium aluminum hydride hydrolyzed. The mixture was filtered and the residue was washed several times with THF. The combined filtrate was collected and dried over magnesium sulfate. After filtration and removal of the solvent afforded 2.84 g (yield: 90%) of compound **7** as white crystals. Mp: 126.0−127.0 °C. ^{1}H NMR ($CDCl_3$, 300 MHz, ppm): δ 7.68−7.65 (d, 2H), 7.33 (s, 2H), 7.31 (s, 2H), 4.77 (s, 4H), 2.12 (s, 6H), 1.97−1.92 (m, 4H, J = 4.11 Hz), 1.24−1.03 (m, 20 H), 0.83−0.79 (t, 6H, J = 6.83 Hz), 0.62−0.59 (br, 4H). Anal. Calcd for $C_{31}H_{46}O_2$: C, 82.61; H, 10.29. Found: C, 82.10; H, 10.18.

2,7-Diformyl-9,9′-dioctylfluorene, 8.[14] Compound **7** (2.70 g, 6 mmol), pyridium chlorochromate (PCC) (5.25 g, 24 mmol), freshly dried 4 Å molecular sieves (1.0 g), and silica gel (1.0 g) were mixed together with dry methylene chloride (100 mL). The mixture was cooled to 0 °C in an ice bath and stirred for 4 h, warmed to room temperature, and stirred for another 12 h. TLC monitoring indicated that the diol compound had been completely converted to the diformyl product. The mixture was run through a short silica gel column eluted with methylene chloride. Removal of the solvent afforded 2.56 g (yield: 95%) of compound **8** as light yellow crystals. Mp: 47.2−48.0 °C. ^{1}H NMR ($CDCl_3$, 300 MHz, ppm): δ 10.10 (s, 2H), 7.93−7.91 (m, 6H), 2.09−2.04 (m, 4H, J = 4.22 Hz), 1.22−1.07 (m, 20H), 0.82−0.80 (t, 6H, J = 6.84 Hz), 0.56−0.53 (br, 4H). Anal. Calcd for $C_{31}H_{42}O_2$: C, 83.36; H, 9.48. Found: C, 82.60; H, 8.86.

2,7-Diiodo-9,9′-dioctylfluorene, 9.[15] A mixture of 9,9-dioctylfluorene (1.95 g, 5 mmol), KIO_3 (0.42 g, 2 mmol), I_2 (1.36 g, 5.42 mmol), and 20% H_2SO_4 (5 mL) in AcOH (50 mL) was heated at 80 °C overnight. When cooled to room temperature, water (100 mL) was added. The whole mixture was neutralized with 2 M Na_2CO_3 and extracted with ether. The organic extracts were washed with brine and dried over magnesium sulfate. After removal of the solvent, the product was purified by recrystallization twice from ethanol to afford 2.40 g (yield: 75%) of compound **9** as a white solid. Mp: 55.1−56.0 °C. ^{1}H NMR ($CDCl_3$, 300 MHz, ppm): δ 7.66−7.63 (m, 4H), 7.41−7.39 (m, 2H), 1.90 (t, 4H), 1.20−0.81 (br, 24H), 0.60 (t, 6H). Anal. Calcd for $C_{29}H_{40}I_2$: C, 54.21; H, 6.23; I, 39.60. Found: C, 54.05; H, 6.30; I, 38.21.

2,7-Bis[(trimethylsilyl)ethynyl]-9,9′-dioctylfluorene, 10.[16] 2,7-Diiodo-9,9-dioctylfluorene (3.21 g, 5 mmol), bis(triphenylphosphine)palladium dichloride (197.5 mg, 0.25 mmol), and copper iodide (47.5 mg, 0.25 mmol) were mixed with piperidine (30 mL). Trimethylsilyl acetylene (1.08 g, 11 mmol) was slowly added to the mixture at room temperature. The reaction temperature was then slowly increased and the reactant was refluxed for 6 h. The solvent was stripped off under reduced pressure. The residue was passed through a short column of silica gel using toluene as the eluent. Evaporation of the solvent led to a brown oil which crystallized upon standing. Twice recrystallization from ethanol yielded 0.94 g (yield: 32%) of compound **10** as white crystals. Mp: 89.3−89.9 °C. ^{1}H NMR ($CDCl_3$, 300 MHz, ppm): δ 7.60−7.57 (d, 2H, J = 7.24 Hz), 7.76−7.43 (dd, 2H, J = 7.83 Hz, J = 1.41 Hz), 7.40 (s, 2H), 1.95−1.89 (m, 4H, J = 4.12 Hz), 1.22−1.02 (m, 20H), 0.76 (t, 6H, J = 6.84 Hz), 0.56 (m, 4H), 0.28 (s, 18 H). Anal. Calcd for $C_{39}H_{58}Si_2$: C, 80.34; H, 10.03; Found: C, 80.32; H, 9.88.

2,7-Diethynyl-9,9′-dioctylfluorene, 11.[17] Methanol (45 mL) and aqueous potassium hydroxide (4 mL, 20%) were added at room temperature to a stirred solution of 2,7-bis[(trimethylsilyl)ethynyl]-9,9′-dioctylfluorene (2.54 g, 4.36 mmol) in THF (80 mL). The reactant was left at room temperature for 10 h. It was then poured into water (20 mL) and extracted three times with ether. The combined organic extracts were dried over anhydrous magnesium sulfate and then filtered. The solvent was stripped off to obtain a viscous liquid, which was then refined using a silica gel column with hexane as the eluent followed by recrystallization in ethanol to give 1.55 g (yield: 82%) of compound **11** as light yellow crystals. Mp: 36.0−36.5 °C. ^{1}H NMR ($CDCl_3$, 300 MHz, ppm): δ 7.65−7.62 (d, 2H), 7.50−7.47 (d, 2H), 3.15 (s, 2H), 1.98−1.92 (m, 4H), 1.23−1.10 (m, 20H), 0.86−0.81 (t, 6H, J = 6.74 Hz), 0.62 (m, 4H). Anal. Calcd for $C_{33}H_{42}$: C, 90.35; H, 9.66. Found: C, 90.90; H, 9.39.

Poly[2,7-(9,9′-dioctylfluorene)-*co*-*alt*-5,5′-(2,2′-bipyridine)], P1.[18] To a mixture of 9,9-dioctylfluorene-2,7-bis(trimethylene boronate) (534 mg, 0.96 mmol), 5,5′-dibromo-2,2′-bipyridine (301 mg, 0.96 mmol) and tetrakis(triphenylphosphine) palladium [$Pd(PPh_3)_4$] (20 mg) was added a degassed mixture of toluene (6 mL) and 2 M potassium carbonate aqueous solution (3 mL). The mixture was vigorously stirred at 85−90 °C for 48 h under the protection of nitrogen. After the mixture cooled to room temperature, it was poured into a stirred mixture of methanol and deionized water (10:1). A fibrous solid was obtained by filtration. It was washed with methanol, water and methanol, successively. The polymer was further purified by washing with acetone in a Soxhlet apparatus for 24 h to remove oligomers and catalyst residues, and was dried under reduced pressure at room temperature to afford 490 mg (yield: 86%) of **P1** as an off-white fibrous solid. ^{1}H NMR ($CDCl_3$, 300 MHz, ppm): δ 9.07 (br, 2H), 8.63 (br, 2H), 8.19 (br, 2H), 7.91 (br, 2H), 7.68 (br, 4H), 2.11 (br, 4H), 1.21−0.79 (m, 30H). ^{13}C NMR ($CDCl_3$, 75.5 MHz, ppm): δ 152.18, 147.27 (m), 140.74, 137.07, 136.32 (m), 135.58 (m), 126.10, 121.51, 120.62, 55.50, 40.33, 31.42, 30.58, 29.02, 29.00, 23.82, 22.49, 13.88. FT-IR (KBr, cm^{-1}): 3035, 3010, 2929, 2856, 1895, 1590, 1536, 1486, 1455, 1366, 1254, 1223, 1131, 1065, 1015, 930, 888, 845, 818, 784, 745, 722, 629, 552, 405. Anal. Calcd for $C_{39}H_{46}N_2$: C, 86.35; H, 8.49; N, 5.17. Found: C, 85.56; H, 8.06; N, 6.06.

Poly[9,9′-dioctylfluoren-2,7-ylenevinylene-*co*-*alt*-5,5′-(2,2′-bipyridylenevinylene)], P2.[12] A solution of 5,5′-bis-(diethylphosphinatylmethyl)-2,2′-bipyridine (228 mg, 0.5 mmol) and 2,7-diformyl-9,9′-dioctylfluorene (223 mg, 0.5 mmol) in dry THF (35 mL) was stirred at room temperature under argon. Potassium *tert*-butoxide (1.0 M in THF solution, 2 mL) was added dropwise, and the reaction mixture was continuously stirred for 4 h at room temperature. It was poured into methanol (250 mL) with stirring. The precipitate was collected by filtration. The crude polymer was thoroughly washed in a Soxhlet apparatus with methanol, acetone, and then THF. The THF soluble portion was then precipitated again in methanol. After filtration and drying under vacuum, 85 mg (yield: 29%) of **P2** was obtained as a fibrous light yellow solid. ^{1}H NMR ($CDCl_3$, 300 MHz, ppm): δ 8.84 (br, 2H), 8.48 (br, 2H), 8.04 (br, 2H), 7.71 (br, 2H), 7.54 (br, 4H), 7.27−7.26 (m, 2H), 2.04 (br, 4H), 1.10−0.78 (m, 30H). FT-IR (cm^{-1}): 3034, 3011, 2922, 2852, 1895, 1629, 1590, 1540, 1470, 1378, 1351, 1281, 1254, 1196, 1131, 1054, 1019, 1003, 957, 888, 857, 830, 807, 741, 645, 537, 405. Anal. Calcd for $C_{43}H_{50}N_2$: C, 86.87; H, 8.42; N, 4.71. Found: C, 86.40; H, 7.95; N, 4.60.

Poly[9,9′-dioctylfluoren-2,7-yleneethylene-*co*-*alt*-5,5′-(2,2′-bipyridylethylene)], P3.[17] 2,7-Diethynyl-9,9′-dioctylfluorene (399 mg, 0.91 mmol), 5,5′-dibromo-2,2′-bipyridine (258 mg, 0.82 mmol), bromobenzene (28.5 mg, 18.2 mmol), tetrakis-(triphenylphosphine) palladium [$Pd(PPh_3)_4$] (42 mg), and cuprous iodide (8 mg) were combined in degassed toluene (25 mL) and diisopropylamine (10 mL). After the reaction mixture was stirred at 70 °C for 24 h, bromobenzene (0.16 g, 1 mmol) was added for end-capping the polymer for an additional 2 h. After the reaction mixture cooled to room temperature, it was poured into methanol (300 mL). The precipitate was filtered, dissolved in chloroform, and precipitated again in methanol to obtain a fibrous solid. After washing with methanol, water, and methanol, successively, the polymer was further purified by washing with acetone in a Soxhlet apparatus for 24 h to remove oligomers and catalyst residues. Dried under vacuum at room temperature afforded 348 mg (yield: 72%) of **P3** as a fibrous light yellow solid. ^{1}H NMR ($CDCl_3$, 300 MHz, ppm): δ 8.88 (br, 2H), 8.49 (br, 2H), 7.98 (br, 2H), 7.73 (br, 2H), 7.52

(br, 4H), 2.11 (br, 4H), 1.21−0.79 (m, 30H). ^{13}C NMR ($CDCl_3$, 75.5 MHz, ppm): δ 151.21, 141.04, 139.25, 137.48, 130.91, 128.28, 126.01, 121.31, 120.65 (m), 120.12, 94.90, 86.80, 55.30, 40.22, 31.67, 30.79, 29.87, 29.10, 23.64, 22.48, 13.95. FT-IR (cm^{-1}): 3065, 3024, 2926, 2852, 1895, 1606, 1463, 1416, 1378, 1262, 1208, 1131, 1003, 888, 818, 753, 722, 631, 595, 524, 500. Anal. Calcd for $C_{43}H_{46}N_2$: C, 87.41; H, 7.78; N, 4.74. Found: C, 86.13; H, 7.66; N, 4.24.

Results and Discussion

Synthesis and Characterization. The basic strategies employed for the synthesis of **P1**, **P2**, and **P3** are based on the Suzuki reaction,[18] the Wittig−Horner reaction,[12] and the Heck reaction,[17] respectively. The synthetic routes to all of the three polymers and the corresponding monomers are illustrated in Scheme 1. Compound **1** was synthesized via a modified Burstall procedure by direct bromination of 2,2′-bipyridine hydrobromide salt with liquid bromine in a sealed tube, with a yield of 35% after purification.[9] The intermediate **2** was synthesized in 24% yield through self-coupling of 3-picolines catalyzed by the Raney nickel,[10] with the key step in the preparation of high reactivity Raney nickel as the catalyst. Bromination of compound **2** with NBS in the presence of BPO afforded **3** with a yield of 45% after recrystallization from chloroform.[11] The monomer for **P2**, compound **4**, was obtained via the reaction of compound **2** in an excess of triethyl phosphite with a yield of 80%.[12] Direct synthesis of dialdehyde **8** from 9,9-dioctylfluorene or intermediate **5** was unsuccessful in our hands.[19,20] Alternatively, we used an acetylation−reduction−oxidation sequence to execute this transformation. Bromomethylation of 9,9-dioctylfluorene provided the key intermediate **5**, which upon esterification, afforded compound **6** with a yield of 32%. As for the key monomer of **P3**, compound **11** was prepared from 2,7-diiodo-9,9′-dioctylfluorene and trimethylsilyl acetylene by a palladium(II)-catalyzed cross-coupling reaction and the subsequent cleavage of the trimethylsilyl protecting group under base treatment.[21] The polymerization of **P1** depicted in Scheme 1 is based on the Suzuki coupling reaction,[18] which was carried out in a mixture of toluene and aqueous potassium carbonate solution (2 M) containing 1 mol % $Pd(PPh_3)_4$ under vigorous stirring at 85−90 °C for 3 days. **P2** was prepared via the Wittig−Horner condensation reaction[12] between the dialdehyde **8** and the bipyridine diphosphonate **4** in tetrahydrofuran (THF) by slowly adding 2 equiv of a solution of *t*-BuOK (1.0 M in THF) as a base. Also as depicted in Scheme 1, **P3** was prepared by palladium-catalyzed cross-coupling condensation, known as the Heck reaction,[17,21] between an aryl acetylene **11** and an aryl bromide **1**, according to the procedure by Yamamoto et al.[22] It was end-capped with phenyl groups, which also enabled a straightforward determination of the molecular weight by ^{1}H NMR spectroscopy.[23] All three polymers were obtained with satisfactory yields. After purification and drying, **P1**, **P2**, and **P3** were obtained as off-white, light yellow, and light yellow fibrous solids, respectively. All these polymers readily dissolve in common organic solvents, such as chloroform, THF, toluene and xylene. The number-average molecular weights (M_n) of the polymers were determined by gel permeation chromatography (GPC) against the polystyrene standards to be 35 200 to 59 200 with the polydispersity index of around 2.0 (see Table 1). The chemical structures of the polymers were verified by ^{1}H NMR, ^{13}C NMR, FT-IR, and elemental analyses.

Scheme 1. Synthetic Routes for the Monomers and Polymers[a]

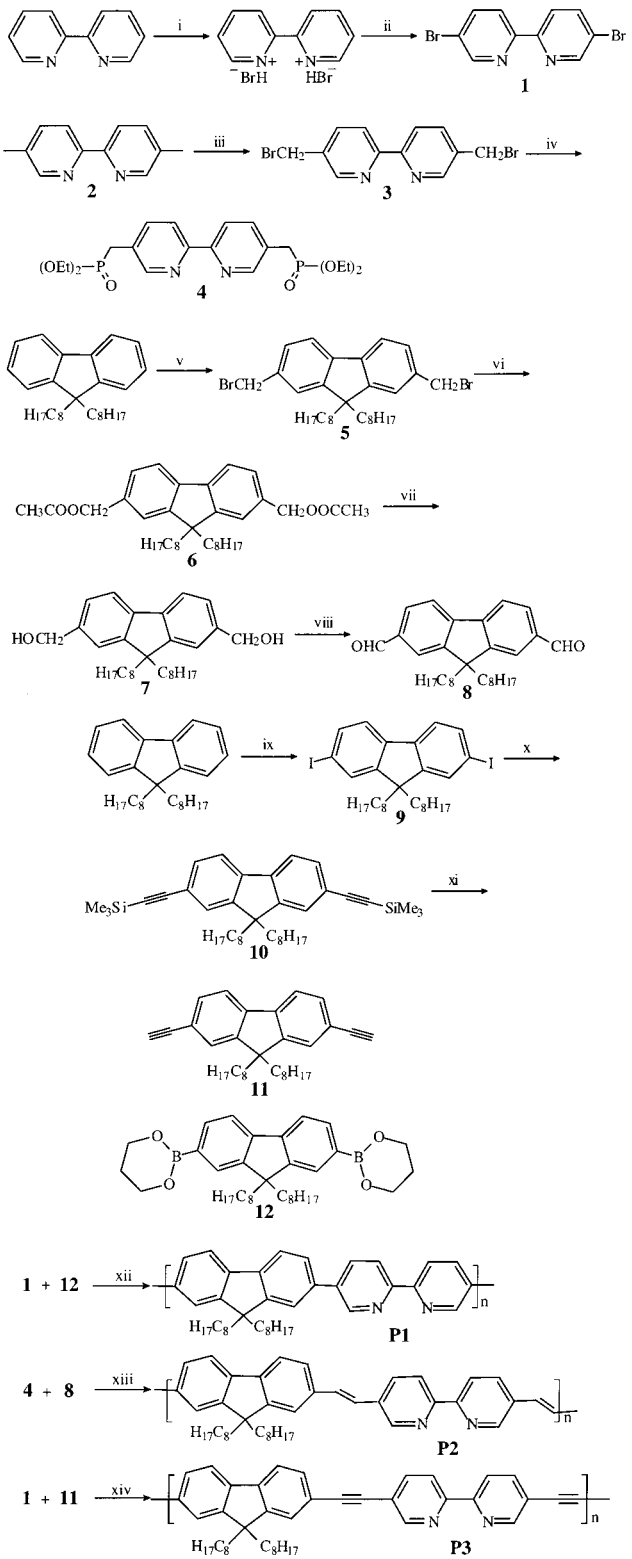

[a] Reagents and conditions: (i) HBr (g), MeOH, room temperature, 1 h; (ii) Br_2 (liquid), sealed tube, 180 °C, 72 h; (iii) NBS, BPO, CCl_4, reflux, 5 h; (iv) Triethyl phosphite, reflux, 4 h; (v) $(CH_2O)_n$, 30% HBr in acetic acid, 60 °C, 24 h; (vi) KOAc, $(CH_3CO)_2O$, CH_3COOH, reflux, 24 h; (vii) $LiAlH_4$, THF, reflux, 8 h; (viii) PCC, CH_2Cl_2, room temperature, 12 h; (ix) KIO_3, I_2, 20% H_2SO_4, CH_3COOH, 80 °C, 24 h; (x) $(PPh_3)_2PdCl_2$, CuI, $(CH_3)_3SiCCH$; (xi) KOH, CH_3OH−THF; (xii) $[(PPh_3)_4]Pd^0$ 1.0 mol %, toluene/2 M K_2CO_3 (3:2), 85 °C, 48 h; (xiii) *t*-BuOK, THF, room temperature, 4 h; (xiv) $[(PPh_3)_4]Pd^0$, CuI, toluene/diisopropylamine (2.5:1), 70 °C, 24 h.

Table 1. Number-Average (M_n) and Weight-Average (M_w) Molecular Weights of the Polymers

polymer	M_n	M_w	M_w/M_n
P1	35 200	56 975	1.57
P2	37 200	55 300	1.49
P3	59 200	113 500	1.92

Figure 1 displays the ^{1}H NMR spectra of **P1**, **P2**, and **P3**. There are five peaks in the aromatic region for **P1**. The three peaks in the lower field at 9.07, 8.63, and 8.18 ppm are attributed to the three kinds of different protons on the bipyridine ring. The other peaks between 7.89 and 7.68 ppm belong to the protons on the fluorene ring. The aromatic region of **P2** is similar to that of **P1**, with all of the peaks slightly shifted by 0.1−0.2 ppm to the higher field. There are two sets of new peaks appearing around 7.25 ppm for **P2**, which can be assigned as the vinylic proton peaks. Compared with the spectrum of **P1**, the aromatic peaks for **P3** have also shifted to a slightly higher field, with a new peak appearing around 7.35 ppm, which is due to the end-capping benzene group. FT-IR studies reveal that all three polymers give characteristic peaks in the range of 1420−1500 cm^{-1}, which are due to from bipyridine and benzene rings. For **P2**, there is a sharp absorption at 957 cm^{-1}, corresponding to the out-of-plane bending mode of the *trans*-vinylene groups, indicating that the newly formed vinylene double bonds are mainly in the trans configuration. There is no residue peak around 1680 cm^{-1}, indicative of a relatively high molecular weight for the polymer synthesized via the Wittig−Horner reaction.

Thermal stability of the polymers in nitrogen was evaluated by thermogravimetric analysis (TGA). The polymers showed weight loss starting at 379 °C for **P1**, 380 °C for **P2**, and 350 °C for **P3**, respectively, indicative of good thermal stability. Thermally induced phase transition behavior of the polymers was also investigated with differential scanning calorimetry (DSC) in a nitrogen atmosphere. **P1** exhibited a clear glass transition starting at ∼105 °C. In comparison with **P1**, the glass transition temperature (T_g) of **P2** was decreased by ∼20 °C to 82 °C. We could not observe the T_g for **P3**. The relatively high glass transition temperatures are essential for many applications, such as in light-emitting diodes as emissive materials.[24]

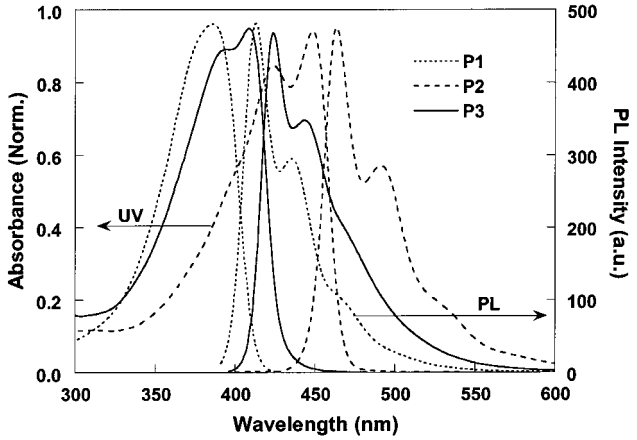

Figure 2. UV−visible absorption spectra and photoluminescence spectra of **P1**−**P3** measured from the THF solutions (∼5.0 × 10^{-6} M) at room temperature.

Optical Properties. The spectroscopic properties of **P1**−**P3** were measured both in solution (THF) and in thin films (spin-cast from chloroform solutions). The UV−visible absorption and photoluminescence (PL) spectra of **P1**−**P3** in THF (ca. 1 × 10^{-5} M) are shown in Figure 3. **P1** exhibited the absorption maximum at 386 nm. Its PL spectrum peaked at 413 nm with a shoulder around 435 nm. In comparison with **P1**, **P2** had shown an obvious spectral red shift, both in absorption (Δ = 62 nm) and in emission (Δ = 52 nm). This obvious spectral difference could be understood in terms of the better conjugation along the polymer main chain due to the inserting of the vinylene unit, which increased the effective conjugation length, and hence leading to the spectral red shift. Both the UV and PL spectra of **P3** were red shifted as compared to those of **P1**, while they bore resemblance shapes to that of **P2.** This spectral red shift may be explained by the improved π-overlap due to the accommodating nature of the acetylene unit.[25] However, both of the spectra were blue shifted as compared to that of **P2**, which was similar to the previous observations that the wavelengths of the electronic absorption maxima (λ_{max}) of the PE compounds were shorter than those of the PV analogues.[26] Some theoretical and experimental results indicated that the double bond allows better electron

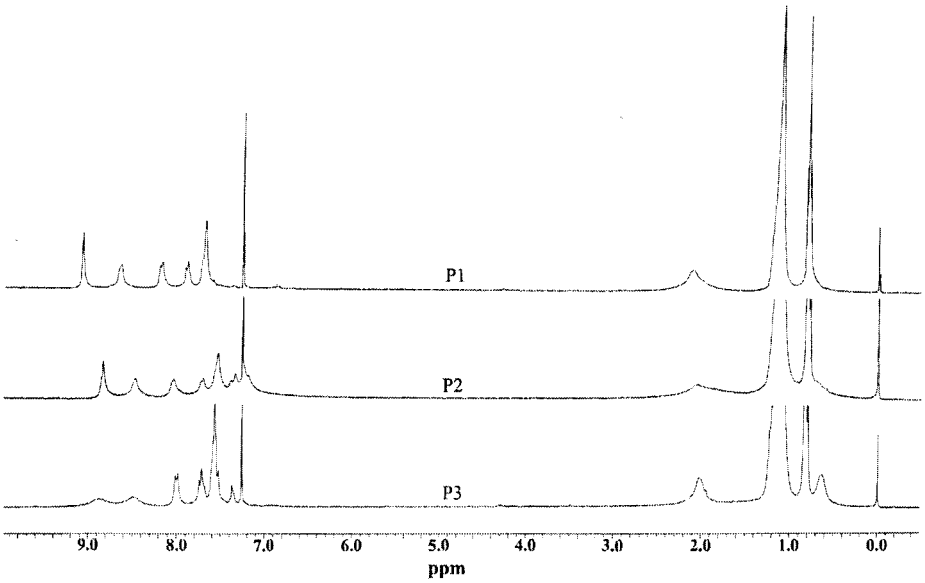

Figure 1. ^{1}H NMR spectra of **P1**−**P3**.

Table 2. Optical and Electrochemical Data of P1−P3

	λ_{max}(solution)[a] (nm)		λ_{max}(films)[a] (nm)			*p*-doping[c] (V)			*n*-doping[c] (V)		
polymer	abs	em	abs	em	E_g[b] (eV)	E_{onset}	E_{pa}	E_{pc}	E_{onset}	E_{pc}	E_{pa}
P1	385	413 (435)	383	453, 477 (425)	2.88	1.39	1.65	1.67	−1.76	−1.98	−1.88
P2	448 (424)	463 (492)	432 (459)	521	2.52	1.01	1.25		−1.60	−1.75	−1.83
P3	409 (392)	424 (444)	425 (395)	477, 503 (439)	2.74	1.50	1.69		−1.67	−2.00	−1.83

[a] The data in parentheses are the wavelengths of shoulders and subpeaks. [b] E_g stands for the band gap energy estimated from the onset wavelength of the optical absorption. [c] E_{pa} and E_{pc} stand for anodic peak potential and cathodic peak potential, respectively.

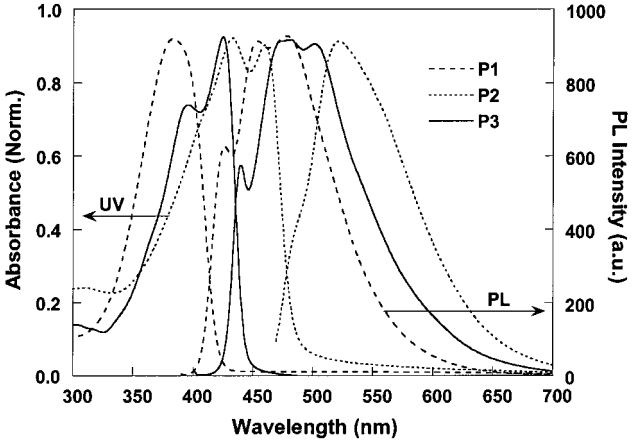

Figure 3. UV−visible absorption spectra and photoluminescence spectra of **P1**−**P3** measured from the spin-coated films on quartz plates at room temperature.

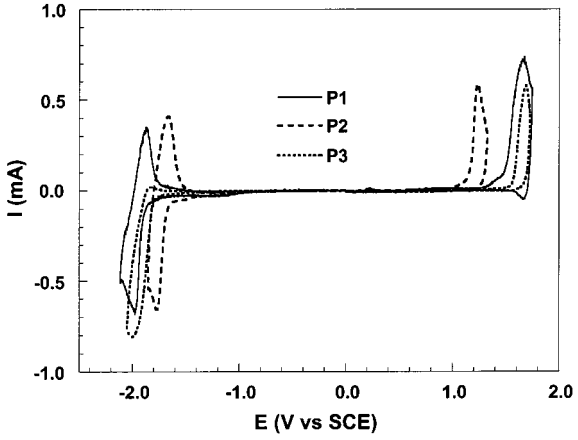

Figure 4. Cyclic voltammograms of **P1**−**P3** films coated on platinum plate electrodes in acetonitrile containing 0.1 M Bu_4NClO_4. Counter electrode: platinum wire. Reference electrode: $Ag/AgNO_3$ (0.10 M in acetonitrile). Scan rate: 50 mV/s.

delocalization than the triple bond.[26] We may suppose that the spectral blue shift here could be explained by the lesser electron delocalization through the triple bond in **P3** than that of the double bond in **P2**.

The Stokes shifts between the absorption and emission of these three polymers are relatively small, reflecting the rigid geometry of the conjugated main chain structures.[27] There are great differences between the Stokes shifts of the three polymers. **P1** had a Stokes shift of 28 nm, which was almost twice that of **P2** and **P3**. Usually the Stokes shift comes from two sources: emission either from the excited segments of a conjugated polymer undergoing a deformation into more planar conformation along the chain or from the migrated excitons in other segments where ring rotations are not hindered.[28] It is expected that our designed polymer with vinylene (**P2**) or ethylnylene unit (**P3**) inserted into the polymer main chain had caused more rigid structures than **P1** due to a much smaller Stokes shift.

Transparent and uniform films of the polymers were prepared on quartz plates by spin-casting their solutions in chloroform at room temperature. The film of **P1** emitted intensive blue light by the excitation of UV light. The **P2** film emitted green light, while the emissive color of **P3** film was blue. The relatively identical absorption spectra of **P1** in solution and **P1** as a solid film indicated that there was little difference in the conformations of the polymer in the two states. However, the emission spectra of the polymer in solution and as a solid film were quite different. In comparison with its solution emission at 413 nm, the main emission peak in the solid films shifted about 40 nm toward the longer wavelength with a broadened peak shape. This may be due to the intrachain and/or interchain interaction at excited states in the solid state. The absorption spectrum of **P2** film onset at 453 nm (band gap, 2.74 eV) with a peak at 432 nm. The emission spectra of **P2** was red shifted about 58 nm as compared to its emission in solution. As for **P3**, which had an absorption spectrum red shifted about 10 nm with respect to its corresponding spectrum in solution, its PL spectrum resembled that of **P1**, with also a slight red shift. The spectroscopic parameters of **P1**, **P2**, and **P3** in film states are summarized in Table 2.

Electrochemical Properties. The electrochemical behavior of the polymers was investigated by the cyclic voltammetry (CV). The CV was performed in a solution of Bu_4NClO_4 (0.10 M) in acetonitrile at a scan rate of 50 mV/s at room temperature under the protection of argon. A platinum electrode (~0.06 cm^2) was coated with a thin polymer film and was used as the working electrode. A Pt wire was used as the counter electrode and an $Ag/AgNO_3$ electrode was used as the reference electrode.

As shown by the cyclic voltammograms in Figure 4, all of the three polymers showed partial reversibility in n-doping processes, while only **P1** had some reversibility for its p-doping process. The corresponding electrochemical data are summarized in Table 2. Comparing with PFs, the reduced electrochemical reversibility of these three polymers could be attributed to the enhancement of electron affinity of the polymers through the introduction of the bipyridine segments, which are electron deficient and prefer n-doping.[29] Taking **P1** for example, we may find that, on sweeping the polymer cathodically, the onset of the n-doping process occurred at the potential of −1.73 V. The cathodic current quickly increased with the reduction peak appeared at −1.98 V and a corresponding reoxidation peak at −1.88 V. The n-doping potential $E_{redn}^{1/2}$ was thus calculated to be −1.93 V. In the anodic scan, the p-doping process onset at 1.39 V, giving a sharp oxidation peak at 1.65 V with a rereduction peak appearing at 1.67 V. Accordingly, the p-doping potential $E_{ox.}^{1/2}$ was determined to be 1.66 V. Comparison of the electrochemical data of **P2** with

Table 3. Absorption Responses of P1−P3 upon Chelating with Metal Ions

		metal ions		
		P1	P2	P3
ion free (λ_{max})		385.5	448	408.5
$\Delta\lambda_{abs}$ (nm)	Ag^+	21.5	39	40.5
	Co^{2+}	25.5	23	20
	Ni^{2+}	30.5	26	26
	Zn^{2+}	38.5	33.5	3[b]
	Fe^{3+}	[a]	26	32.5
	Mn^{2+}	22.5	1	3
	Cu^{2+}	1	0	0
	Cd^{2+}	1	0	0
	Pd^{2+}	9.5	50	0
	Fe^{2+}	1.5	0	0

[a] Overlay of the absorption between the polymer and Fe^{3+} ion in THF. [b] New side peak appeared.

those of **P1** could find an obvious decrease for both the oxidation potential and the reduction potential. Consequently, **P2** had a lower LUMO energy level and a higher HOMO energy level with a band gap about 0.5 eV smaller as compared to that of **P1**. As for **P3**, it had a slight increment (<0.1 V) for both the reduction potential and the oxidation potential than that of **P1**; however, less reversibility was observed for both the n-doping and p-doping processes. Consequently, both the HOMO and LUMO energy levels of **P3** were lower than those of **P1**, although the polymers had a similar band gap. This result is of special interest for the study of the relationship between the polymer main chain structures and the ion sensing sensitivity and selectivity since the sensing sites and the electronic properties of the polymers (**P1** and **P3**) are quite similar. We can attribute the polymer sensing difference of certain ions mainly due to the difference in the rigidity of the main chain structures.

Ion Sensing Properties. The ion responsive properties of the polymers were studied in THF solution at a polymer concentration of 5.0×10^{-6} M. Alkali, alkaline earth, and transition metal ions (1.0 M solution in water) were used in the experiment. All of the three polymers had no response to the addition of alkali metal ions (up to 100 ppm) and alkaline earth metal ions with the exception of Mg^{2+}. However, the polymer solutions were very sensitive to the transition metal ions. The ionochromic effects of the three polymers were characterized by instant color changes from colorless to deep yellow (for **P1** and **P3**), and from yellow to brown red for **P2** upon the addition of metal ions. The spectral shifts were metal ion-dependent. For instance, in the case of **P1**, the absorption maximum ($\Delta\lambda_{max}$) shifts ranged from 9.5 nm, induced by Pd^{2+}, to 38.5 nm, caused by Zn^{2+}. The pristine peak wavelengths in the absorption spectra of the polymer solutions and the corresponding red-shifted wavelengths ($\Delta\lambda_{max}$) upon the addition of different metal ions (100 ppm) are summarized in Table 3. The spectral red shift was attributed to the conjugation enhancement along the polymer backbone induced by the bidentated coordination of metal ions with the 2,2′-bipyridyl units.[7a] For different metal ions, the differences in the changed absorption spectra reflected different coordination ability of metal ions to the 2,2′-bipyridyl units, and stronger coordination induced a larger spectral red shift.

According to the differences in the spectral response, the metal ions could be categorized into three groups. The first group metal ions caused a large red shift (about 20−30 nm), and produced a strong fluorescent quenching. These metal ions include Zn^{2+}, Ni^{2+}, and Co^{2+}. The second group of metal ions, including Mn^{2+}, Pd^{2+}, and Ag^+, also produced an obvious red shift, but just weakly quenched the fluorescence of the polymers. The last group of the metal ions is those which only partially quenched the fluorescence of the polymers without a noticeable absorption red shift. They are Mg^{2+}, Al^{3+}, Cu^{2+}, Cd^{2+}, and Fe^{2+}. It is interesting to find that, for the first group of the metal ions, there was no obvious difference in the red shift value among the three polymers. This maybe due to the strong coordination ability of the metal ions with the bipyridyl unit, which smeared the effect of the joint bonds between the bipyridyl and fluorene units to the enhancement of coplanarity between two pyridyl rings through chelation. As for the ions of the second group, take Mn^{2+} for an example, the addition of Mn^{2+} (100 ppm) caused about 23 ppm red shift for **P1**, while the red shifts observed for **P2** and **P3** were only about 1−3 ppm. For all the metal ions (with the exception for Ag^+), **P1** always had a larger red shift than **P2** and **P3,** which had similar absorption red shifts upon chelating. Since the sensing sites for all of the three polymers were the same, these results revealed that the backbone structures played an important role in the response sensitivity of the polymers to the metal ions. We attribute this phenomenon to the difference of the backbone rigidity of the polymers: higher rigidity presents a bigger hindrance for the coplanarity of the bipyridyl unit caused by the chelation.

More clear evidences of different response sensitivity of **P1**, **P2**, and **P3** to metal ions were observed in the fluorescent changes. The fluorescence of all the three polymers could be completely quenched by $Co^{2+}$and Ni^{2+} at a very low concentration of below 0.1 ppm. This gave an estimation that each ion can effectively "turn off" the fluorescence of ∼50 repeat units in the polymers, implying that a signal amplification through the molecular wire approach was involved.[15] In this case, no obvious difference in the ion sensitivity among the three polymers was exhibited, probably due to the strong chelation of the polymers to the ions, which was coincident with the observation in the absorption spectra. For all the metal ions in the second and third groups, we found that **P1** was the easiest to be fluorescently quenched by metal ions, whereas **P3** always had the poorest response to metal ions. For instance, the concentrations of Mn^{2+} for totally quenching the fluorescence of the polymer solutions are 3 ppm for **P1**, 10 ppm for **P2**, and 100 ppm for **P3**. The PL spectral changes of **P1** upon the addition of Mn^{2+} is shown in Figure 5, and the corresponding titration curves for all of the three polymers are depicted in Figure 6. As shown in Figure 7, the molecular structure-dependent response of the polymers to metal ions was more apparent in Al^{3+}. The addition of 0.1 ppm of Al^{3+} may quench about 40% of the fluorescence of **P1**. At the same conditions, the quenching ratio was about 16% for **P2**, while **P3** had no response even when the ion concentration reached 100 ppm.

The spectral response of 2,2′-bipyridyl-containing conjugated polymers to metal ions is believed to be based on the chelation between the 2,2′-bipyridyl units and the metal ions, which induces the conformation change (more conjugated) and the variation of electron density of polymer chains.[7a,8] Given the fact that the

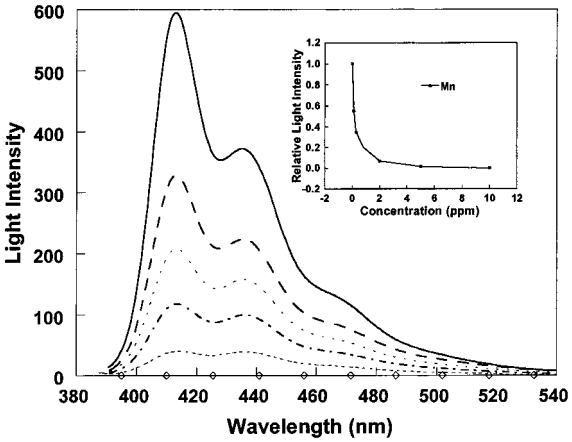

Figure 5. Fluorescence spectra of **P1** in THF upon adding different amount of Mn^{2+} ($MnCl_2$). Inset: Titration curves of Mn^{2+} to **P1** in THF solution.

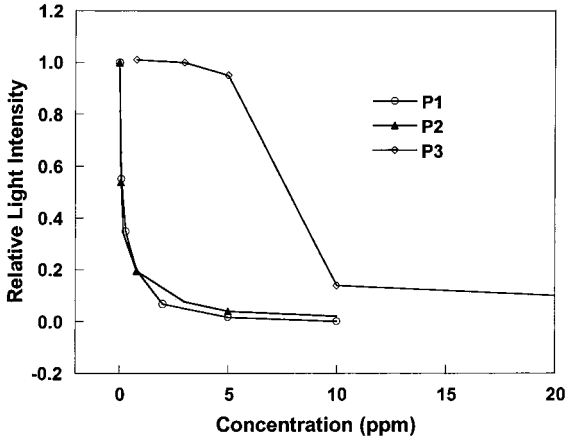

Figure 6. Titration curves of Mn^{2+} to **P1**−**P3**. Concentration of the polymer solution: 5.0×10^{-6} M.

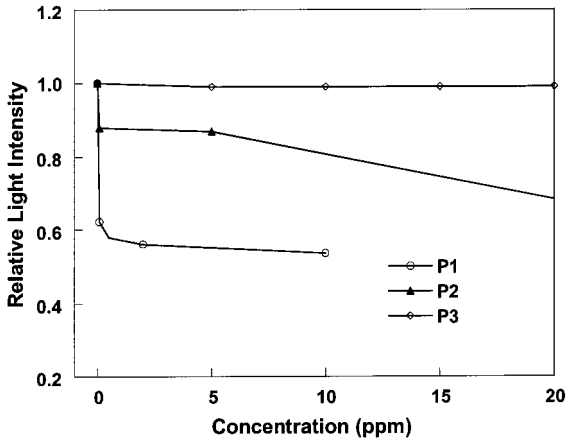

Figure 7. Titration curves of Al^{3+} to **P1**−**P3**. Concentration of the polymer solution: 5.0×10^{-6} M.

two pyridine rings in a 2,2′-bipyridyl unit are not coplanar, but with a 20° dihedral angle in its transoid-like conformation, [7a] effective chelation may force the two pyridine rings to be more coplanar. Consequently, more or less absorption red shifts were observed in the polymers upon chelating with certain metal ions. Because the 2,2′-bipyridyl moiety is a part of the repeat unit in all the three polymers, when the two pyridine rings become more coplanar by chelation, the coplanarity must be affected by the bonds which link the fluorene and 2,2′-bipyridyl units. A weak restriction allows the coplanarity of a 2,2′-bipyridyl unit to happen easier and thus to chelate metal ions more effectively, which corresponds to a stronger spectral response. It is also easy to understand that such a difference in chelation caused by the different linking bonds will be more pronounced in the interaction with the metal ions which have a weaker coordinating ability with 2,2′-bipyridyl moieties. Our experimental results implied that the single C−C bond between the fluorene unit and the 2,2′-bipyridyl unit (**P1**) provided the weakest forbiddance for the chelation of 2,2′-bipyridyl unit with metal ions, which was followed by the vinylene bond (**P2**), and the ethynylene linker presented the highest resistance for the coplanarity of 2,2′-bipyridyl unit. This phenomenon may be associated with the difference in the rigidity of the polymers, as suggested by the observed differences in their Stokes shifts.

Summary

Three alternating polymers based on 2,2′-bipyridyl and fluorene were synthesized, in which the 2,2′-bipyridyl and fluorene units were linked by a single C−C bond, a vinylene bond, and an ethynylene bond, respectively. The different structures arising from the linkers not only offered different electronic and physical properties of the resulting polymers but also provided us the opportunity to study the effect of the linkers on the spectral response to metal ions by using the 2,2′-bipyridyl unit as the sensing site. All three polymers were responsive to a wide variety of transition metal ions by an absorption spectral red shift and fluorescence quenching. A clear difference in the response sensitivity was observed among the three polymers. It is assumed that the C−C single bond linker (**P1**) provides the weakest resistance (higher backbone flexibility) to the coplanarity of the two pyridine rings of 2,2′-bipyridyl unit during the chelation with metal ions, and thus gives the highest sensitivity to response metal ions. However, the ethynylene linker (**P3**) presents the highest resistance (higher backbone rigidity) to the coplanarity and results in the poorest response sensitivity to metal ions. The difference of backbone rigidity in the three polymers is supported by the difference of their Stokes shifts in solution. The results reveal a clear guidance for the molecular design toward the conjugated polymer-based chemosensors by using 2,2′-bipyridyl as the recognition site: a C−C single bond linker between conjugated units (compared with vinylene and ethynylene linkers) and lower backbone rigidity give higher response sensitivity.

References and Notes

(1) Leonid, M. G.; Martin, R. B.; Michael, C. P. *J. Mater. Chem.* **1999**, *9*, 1957.
(2) Crawford, K. B.; Goldfinger, M. B.; Swager, T. M. *J. Am. Chem. Soc.* **1998**, *120*, 5187.
(3) (a) de Silva, A. P.; Gunaratne, H. Q. N.; Gunnlaugsson, T.; Huxley, A. J. M.; McCoy, C. P.; Rademacher, J. T.; Rice, T. E. *Chem. Rev.* **1997**, *97*, 1515. (b) Fluorescent Chemosensors for Ion and Molecule Recognition. *ACS Symp. Ser.* **1993**, 538.
(4) McQuade, D. T.; Pullen, A. E.; Swager, T. M. *Chem. Rev.* **2000**, *100*, 1537.
(5) (a) Zhou, Q.; Swager, T. M. *J. Am. Chem. Soc.* **1995**, *117*, 12593. (b) Swager, T. M. *Acc. Chem. Res.* **1998**, *31*, 201.
(6) (a) Yamamoto, T.; Omote, M.; Miyazaki, Y.; Kashiwazaki, A.; Lee, B. L.; Kanbara, T.; Osakada, K.; Inoue, T.; Kubota, K. *Macromolecules* **1997**, *30*, 7158. (b) Scheib, S.; Bäuerle, P. *J. Mater. Chem.* **1999**, *9*, 2139. (c) Marsella, M. J.; Swager, T. M. *J. Am. Chem. Soc.* **1993**, *115*, 12241. (d) McCullough, R. D.; Tristram-Nagle, S.; Williams, S. P.; Lowe, R. D.; Jayara-

man, M. *J. Am. Chem. Soc.* **1993**, *115*, 4910. (e) McCullough, R. D.; Williams, S. P. *J. Am. Chem. Soc.* **1993**, *115*, 11608.
(7) (a) Wang, B.; Wasielewski, M. R. *J. Am. Chem. Soc.* **1997**, *119*, 12. (b) Kimura, M.; Horai, T.; Hanabusa, K.; Shirai, H. *Adv. Mater.* **1998**, *10*, 459.
(8) Chen, L. X.; Jäger, W. J. H.; Gosztola, D. J.; Niemczyk, M. P.; Wasielewski, M. R. *J. Phys. Chem. B* **2000**, *104*, 1950.
(9) Francisco, M.; Raymond, Z. *Tetrahedron Lett.* **1995**, 6471.
(10) Sasse, W. H. F. *J. Chem. Soc.* **1959**, 3046.
(11) Ebmeyer, F.; Vogtle, F. *Chem, Ber.* **1989**, *122*, 1725.
(12) Peng, Z. H.; Gharavi, A. R.; Yu, L. P. *J. Am. Chem. Soc.* **1997**, *119*, 4622.
(13) Cho, H. N.; Kim, J. K.; Kim, D. Y.; Kim, C. Y. *Macromol. Symp.* **1997**, *125*, 133.
(14) Chen, Z. K.; Meng, H.; Lai, Y. H.; Huang, W. *Macromolecules* **1999**, *32*, 4351.
(15) Bao, Z. N.; Chen, Y. M.; Cai, R. B.; Yu, L. P. *Macromolecules* **1993**, *26*, 5281.
(16) Kim, D. Y.; Hong, J. M.; Kim, J. K.; Cho, H. N.; Kim, C. Y. *Macromol. Symp.* **1999**, *143*, 221.
(17) Weder, C.; Wrighton, M. S. *Macromolecules* **1996**, *29*, 5157.
(18) Miyaura, N.; Suzuki, A. *Chem. Rev.* **1995**, *95*, 2457.
(19) Campaigne, E.; Archer, W. L. *Org. Synth. IV*, 331.
(20) Angyal, S. J. In *Organic Reactions*; Adams, R., Blatt, A. H., Cope, A. C., Curtin, D. Y., McGrew, F. C., Niemann, C., Eds.; John Wiley & Sons: New York, 1954; Vol. 8, p 197.
(21) Heck, R. F. *Palladium Reagents in Organic Synthesis*; Academic Press: New York, 1990.
(22) Sanechika, K.; Yamamoto, T.; Yamamoto, A. *Bull. Chem. Soc. Jpn.* **1984**, *57*, 752.
(23) Swager, T. M.; Gil, C. G.; Wrighton, M. S. *J. Phys. Chem.* **1995**, *99*, 4886.
(24) Tokito, S.; Tanaka, H.; Noda, K.; Okada, A.; Taga, Y. *Appl. Phys. Lett.* **1997**, *70*, 1929.
(25) Grell, M.; bradley, D. D. C.; Ungar, G.; Hill, J.; Whitehead, K. S. *Macromolecules* **1999**, *32*, 5810.
(26) Wu, C. Ph.D. dissertation, Iowa State University, 1997.
(27) Lemmer, U.; Heun, S.; Mahrt, R. F.; Scherf, U.; Hopmeier, M.; Siegner, U.; Göbel; Müllen, K.; Bässler, H. *Chem. Phys. Lett.* **1995**, *240*, 373.
(28) (a) Hernandez, V.; Castiglioni, C.; DelZoppo, M.; Zerbi, G. *Phys. Rev. B* **1994**, *50*, 9815. (b) *Conjugated Polymers*: *The Novel Science and Technology of Highly Conducting and Nonlinear Optically Active Materials*; Bredas, J. L., Silbey, R., Eds.; Kluwer: Dordrecht, The Netherlands, 1991. (c) Bredas, J. L.; Cornil, J.; Heeger, A. J. *Adv. Mater.* **1996**, *8*, 447.
(29) Yamamoto, T.; Maruyama, T.; Zhou, Z.-H.; Ito, T.; Fukuda, T.; Yoneda, Y.; Begum, F.; Ikeda, T.; Sasaki, S.; Takezoe, H.; Fukuda, A.; Kubota, K. *J. Am. Chem. Soc.* **1994**, *116*, 4832.

MA0106651